

Frank Paul Phone:++41 1 635 5175
Department of Geography Fax: ++41 1635 6848
Glaciology and Geomorphodynamics Group E-mail: fpaul@geo.unizh.ch
University of Zurich - Irchel
Winterthurer Strasse 190
CH - 8057 Zurich
Switzerland

Revised version: 9. July 2001

The new remote sensing derived Swiss glacier inventory:

I. Methods

FRANK PAUL, ANDREAS KÄÄB, MAX MAISCH, TOBIAS KELLENBERGER, WILFRIED HAEBERLI

Department of Geography, University of Zürich-Irchel, CH-8057 Zürich, Switzerland

ABSTRACT: A new Swiss glacier inventory is to be compiled from satellite data for the year 2000. The study presented here describes two major tasks: First, an accuracy assessment of different methods for glacier classification with Landsat Thematic Mapper data and a digital elevation model (DEM). Second, the GIS-based methods for automatic extraction of individual glaciers from classified satellite data and the computation of 3-dimensional glacier parameters (such as minimum -, maximum -, and median elevation or slope and orientation) by fusion with a DEM. First results obtained by these methods are presented in Part II to this paper (Kääb and others, this issue). It turns out that thresholding of a ratio image from TM4 and TM5 reveals the best-suited glacier map. The computation of glacier parameters in a GIS environment is efficient and suitable for a worldwide application. The developed methods contribute to the USGS-led GLIMS project which is currently compiling a global inventory of land ice masses within the framework of global glacier monitoring (Haeberli and others, 2000).

INTRODUCTION

The latest Swiss glacier inventory from 1973 was compiled from aerial photography with glacier outlines transferred to topographic maps of the scale 1:25.000 (Müller and others, 1976). Various glacier parameters were deduced by manual planimetry (e.g. area) or manual map measurements (e.g. length, minimum and maximum elevation). Since 1973 significant changes in glaciated area have taken place in the Alps with a pronounced advance period of most mountain glaciers (with a total area in general larger than 1 km²) until about 1985, and a strong retreat thereafter (Herren and others, 1999). To overcome some of the difficulties of the previous inventory (costs, manpower) it was decided to use satellite imagery for creating a new inventory reflecting the conditions in 2000. All necessary glacier parameters are derived within a GIS in combination with a digital elevation model (DEM). In addition, the USGS-led GLIMS project (Global Land Ice Measurements from Space) aims at compiling a global inventory of land ice masses, mainly using data from ASTER and ETM+ multispectral scanners on board the satellites Terra and Landsat 7, respectively (Kargel, 2000). Thus, the new Swiss Glacier Inventory 2000 (SGI 2000) serves as a pilot study for GLIMS, with respect to the image-processing techniques for glacier classification and the GIS-based methods for derivation of glacier parameters.

Another aim of the SGI 2000 is the documentation of the behaviour of small glaciers (with a total area less than 1 km²), a task which can be achieved almost only from satellite imagery (Paul, in press b). In the course of the annual measurements of glacier length changes (officially coordinated in Switzerland since 1894), those small glaciers were hardly considered. Among the sample of 121 glaciers measured today they, account for 24% by number and only 2% by area, while they represent 89% by number and 24% by area in the inventory from 1973 (Müller and others, 1976; Kääb and others, this issue). Hence, a glacier type representing about one fifth by area is not monitored and its behaviour not known. Thus, the complete spatial coverage of satellite imagery enables the monitoring of glaciers of all sizes.

In this study, the results from a comparison of different methods for glacier mapping with Thematic Mapper (TM) data is presented. The accuracy of the TM-derived glacier areas is assessed by comparison with manually-derived outlines from higher resolution satellite imagery (SPOT panchromatic channel). Moreover, the precision of the used DEM with respect to glaciological parameters is evaluated by comparison with a reference DEM directly derived from stereo-photogrammetry. Finally, the principles of the GIS-based extraction of individual glaciers and the calculation of glaciological parameters as used for the SGI 2000 are presented.

REMOTE SENSING OF GLACIERS

Previous applications

The methods for glacier delineation with Landsat TM data used in previous investigations can be divided into 3 distinct groups (Paul, in press a): (1) segmentation of ratio images from various TM band combinations, (2) unsupervised and (3) supervised classification techniques. Method (1) is used, for instance, by Bayer and others (1994) with digital numbers (DN) from TM4 and TM5 as input, or with the planetary reflectance at the satellite sensor of the same bands by Hall and others (1988) or Jacobs and others (1997). Rott (1994) created a glacier mask after the thresholding of a ratio image from TM3 and TM5 but used the atmospherically-corrected spectral reflectance of each channel. Aniya and others (1996) worked with method (2) for classification of the entire South Patagonian Icefield (ISODATA clustering with TM 1, 4, and 5 as input). Method (3) was used by Gratton and others (1990) or Sidjak and Wheat (1999) (Maximum-Likelihood classification). Moreover, the latter authors investigated the use of principal component analysis (PCA) or a natural difference snow index (NDSI). Recently, Serandrei-Barbero and others (1999) created a glacier classification scheme using fuzzy set theory and a DEM within a GIS framework. So far, however, most methods were applied only to a smaller number of glaciers (fewer than 50) and all methods were unable to classify the debris-covered ice of a glacier.

Comparison of different glacier mapping methods from Landsat TM

In this study we apply different glacier mapping methods (see below) to a sub-set of a Landsat TM scene (path: 195, row: 28) from 12. September 1985. The test region (15 by 15 km in size) is located in the 'Weissmies' group in the Saas Valley, Swiss Alps (Fig. 1). This region is typical for glaciated environments in Switzerland. It is characterized by steep relief (altitudinal range 1500 - 4500 m a.s.l.), with cast shadow and debris cover on some glaciers. Together with abundant small snow fields, these three influences on glacier mapping accuracy, known to be critical from previous studies, can be examined in this test region.

In Figure 2a-d we present the results from different glacier mapping methods, comparing two glacier maps at a time in each figure: (a) Segmentation of a ratio image from TM3 / TM5 versus TM4 / TM5 using the DN (Fig. 2a), (b) as (a), but using the spectral reflectance instead of DN (Fig. 2b), (c) an unsupervised ISODATA clustering with 20 classes versus TM4 / TM5 from DN (Fig. 2c), and (d) a supervised Maximum-Likelihood classification with 8 classes versus TM4 / TM5 from DN (Fig. 2d). Further methods were applied (NDSI, PCA, usage of

atmospheric corrected TM bands), but results are not shown because they were less accurate.

A glacier map (black = 'glacier', white = 'other') is created by interactive thresholding of the ratio images for methods (a) and (b). The 20 classes of (c) were separated into 'glacier' and 'other' by visual interpretation. For the Maximum-Likelihood classification (d) training areas in eight classes were chosen: glacier 1 and snow 1 (in sunlight), glacier 2 and snow 2 (in shadow), forest, meadow, terrain and cast shadow. For the final glacier map the latter four were converted to 'other' and the first four classes to 'glacier'. For each of the Figure 2a-d two glacier maps were combined with the following colour scheme: 'glacier' on both maps: light grey, 'glacier' only on the first / second map: black / dark grey and, 'other' on both maps: white. To improve the quality of the classification, a 3 by 3 median filter was applied to all glacier maps before combination. A more detailed analysis of 32 glaciers reveals that the average change in glacier area by the median filter is -0.4%, if glaciers smaller than 0.1 km² were not considered.

All methods other than TM4 / TM5 with DN reveal problems with regions in cast shadow (indicated by arrows in Fig. 2a), where they map too much (Figs. 2a, b, d) or too little (Fig. 2c) glacier area. Additional regions within cast shadow are mapped from both methods displayed in Figure 2b. Small snow fields were especially mapped with the methods displayed in Figure 2c and 2d. The accuracy of all investigated methods could be improved partly by changing the relevant parameters (thresholds, training areas, number of clusters) but at the cost of more incorrect results at other places. All methods fail in detection of debris-covered ice because of the spectral similarity to the surrounding terrain. The accuracy of the glacier classification with segmentation of a TM4 / TM5 ratio image using the raw DN proved to be the best method with respect to glacier areas in cast shadow or assigning snow fields to 'other'.

Accuracy of the best glacier mapping method

To evaluate the accuracy of this best-suited classification method, the TM-derived glacier areas were compared with areas derived manually from a higher resolution Spot Pan scene (10 m). Unfortunately, this scene (path: 55, row: 256, acquired on 17. September 1992) does not cover the 'Weissmies' test area, but it shares a small region with a TM scene (path:195, row: 28), acquired only two days prior to the SPOT scene. Because of the good temporal coincidence another test site (located to the south of the 'Nufenenpass') depicted on both, the TM and SPOT scene, was selected. For 32 glaciers within this site, the automatically TM-derived areas turned out to be 2.3% smaller (on average) than on the manually analysed SPOT image. This deviation is well within the accuracy of the manual glacier delineation regarding small snow patches or the delineation of debris-covered areas. Thus, for debris-free ice, the accuracy of the glacier areas inferred from TM are better than about 3%.

The accuracy is illustrated in Figure 3 for a region of 5 by 7 km in size showing the Cavagnoli Glacier (C) and Basodino Glacier (B). The outline as derived from the TM4 / TM5 glacier mapping method (black) is superimposed on the SPOT scene together with the glacier outline of 1973 (white) from the digitized Swiss glacier inventory. The depicted overlay suggests the following: (1) the TM-derived glacier outlines fit quite well to the visible glaciers, (2) small isolated ice fields are not classified as glaciers, (3) the smallest glaciers shrank through disintegration into snow patches, (4) there is a differentiated retreat of the larger glaciers, and (5) the largest glacier (Basodino) was even larger in 1992 than in 1973.

DIGITAL ELEVATION MODEL

Requirements and possibilities

A DEM has two main functions within SGI 2000: (A) the orthorectification of the satellite imagery, and (B) deriving 3D glacier parameters within a GIS. The orthorectification is mandatory for at least four different tasks: (1) To eliminate the effects of perspective distortion, terrain elevation has to be considered during georectification of imagery of rugged terrain. For

instance, a pixel with a height of 3000 m a.s.l., located 90 km from the nadir point, is shifted by 370 m from its real position in the uncorrected image. (2) The borders between individual glaciers were assigned to the classified TM image from a (georeferenced) vector layer containing digitized glacier basin outlines. (3) Overlay of TM scenes from other years or with scenes from other sensors, and (4) fusion with the DEM itself used to derive glacier parameters. All scenes for SGI 2000 were orthorectified with a set of ground control points to a residual rms-error of about half a pixel, using a DEM with 25 m spatial resolution (SGI 2000 DEM) from the Swiss Federal Office of Topography.

3D glacier parameters, like minimum and maximum elevation, glacier length, the median and 2:1 altitude (ELA), and a detailed hypsography, can be computed automatically with a DEM. Slope and aspect of each glacier can be obtained as an average for the entire glacier or as a percentage of selected zones (e.g. accumulation and ablation area). Moreover, average illumination or the percentage area in cast shadow during a day can be calculated. In this way it is possible to achieve a more thorough understanding of topographic influences on monitored changes in glacier area or length.

Comparison with a reference DEM

To analyse the vertical accuracy of the SGI 2000 DEM, a comparison with a reference DEM directly inferred from stereo-photogrammetry was performed (Kääb, 2001). An illuminated version of the SGI 2000 DEM is shown in Figure 4a for a small area (5.7 by 5.0 km) within the test region. Also indicated are the outlines of 7 glaciers, analysed in the discussion below. Artefacts from the interpolation process between the originally digitized contour lines are visible on the illuminated SGI 2000 DEM. They are notably pronounced in gradient products like slope, as illustrated in Figure 4b, which shows the difference in slope to the reference DEM.

The minimum (maximum) elevation differences are -96 (+74) m for the entire area, with a standard deviation of 8.6 m. The corresponding values for the slope differences are -53 (+60) degrees and 6.6 degrees. In our opinion those deviations are not acceptable for the SGI 2000, but the large differences were mostly found at isolated locations or crests, usually not related to glacier coverage. To estimate the influence of the artefacts on the derived glacier parameters, some of them were calculated for the 7 glaciers indicated in Figure 4a. The average differences of minimum (maximum) elevation are -2.7 (-1.3) m, with a standard deviation of 7.6 (7.4) m. The corresponding values for slope are 1.2 (-2.5) degrees and 2.4 (3.3) degrees. These deviations are acceptable for the glacier parameters in the SGI 2000.

GEOGRAPHICAL INFORMATION SYSTEM

Data Preparations

[In the following all Arc/Info-specific names and commands are printed in *italics*.]

By using an orthorectified glacier map derived from TM and a suitable DEM, 3D glacier parameters can be obtained automatically within a GIS. Before the GIS-based processing was started, all data products were converted into Arc/Info (ESRI, 1999) specific formats and three GIS-related tasks were prepared for the SGI 2000: (1) digitizing of the glacier outlines from the inventory of 1973 into a vector layer, (2) creation of a vector layer with glacier basin boundaries (see below), and (3) calculation of DEM products (e.g. slope, aspect) for obtaining 3D glacier parameters. The glacier outlines were digitized from the original maps (scale 1:25,000) as individual *arcs*, with an average rectification error of each map of about 5 m (rms). The central flow lines and the reconstructed outlines of ca. 1850 were also digitized.

To separate connected glaciers in the classified TM image into individual glaciers, the ice divides between them have to be defined. This is done by on-screen digitizing of a new vector layer (*coverage*) using the digitized Swiss glacier inventory and the classified TM image as background in *arcedit*. Ice divides were taken without modification from the digitized inven-

tory and extended to a closed *polygon* roughly surrounding the glacier. All other glaciers were also surrounded by closed *polygons*, which are large enough to include possible future variations of glacier area. The thick black lines in Figure 5 represent these *polygons*. They are shown together with the digitized glacier areas (in grey). With these pre-defined glacier basins it is also possible to assign an unique ID to glacier groups (see below). A group of glaciers can (A) originate from a single glacier through disintegration over time, (B) already be established in a former inventory or (C) consist of an entire glacier comprised of different streams.

DEM products such as slope or aspect (cf. Tab. 1) were calculated within the digital image processing software. Some DEM products are further converted with short FORTRAN-programs, for example the aspects are classified into 8 sectors. The elevation products (such as median elevation or hypsography) are computed within Arc/Info.

The location of the glacier ID is taken from the revised database of Maisch and others (1999). Because many glaciers have split up during recent years, the location of their ID (assigned in 1973) often lies outside their present outline. Therefore, and to handle groups of glaciers, the ID is assigned to the entire basin. This is done by conversion of the data base table (ID, x-, y-coordinate) to a *point coverage* with *generate* and *intersecting* this *coverage* with the glacier basin *coverage*. Thus, each glacier basin holds the glacier ID in the *attribute table*.

Data flow

The data processing can be separated into a general work flow between three modules and a more specific data flow within each module. The modules are (Fig. 6): (1) the GIS module for calculation of quantities within the GIS (e.g. areas of individual glaciers), (2) the CONV module for conversion and re-calculation of Arc/Info output tables (e.g. glacier areas of two different years into relative changes in area), and (3) the VIS module for creation of graphic files from data files (e.g. with XMGR, GMT or IDL). Each module holds individual programs for individual tasks, and each of which consists of an input, calculation and output part. The different modules can be combined to a complete digital chain with the output from a program in one module as the input for a program in the next module (c.f. Figure 6).

The GIS module is shown in Figure 7 in more detail. Only 3 input layers are needed for the GIS module: (A) the pre-defined glacier basins (vector layer) with assigned glacier IDs, (B) the image with the classified glacier areas from TM (geo-tiff), and (C) the DEM or a product from it (table with header). The calculation section consists of the following steps (numbers refer to Fig. 7): The first step (1) is a raster-vector conversion of the glacier map with *imagegrid* and *gridpoly* into a *coverage*. This glacier *coverage* is then (2) combined with the glacier basin *coverage* with *intersect* to obtain the individual glaciers. Together with *intersect* the glacier basin *coverage* cuts each glacier out of the glacier *coverage* in correspondence with his basin. The *coverage* with the individual glaciers (or a selection of them) is then (3) converted with *polygrid* to a *zonal grid* where each zone corresponds to a glacier. The DEM (or a product of it) is (4) converted with *asciigrid* to a *value grid*, where each cell holds the value of the DEM at that location. The last step (5) is the combination of the *value grid* and the *zonal grid* with *zonalstats*. This command gives for each zone (glacier) statistic parameters (e.g. minimum, maximum, range, mean, standard deviation) according to the underlying *value grid* (elevation in case of the DEM). The resulting output table can be processed further with the CONV and VIS modules.

DISCUSSION AND CONCLUSION

The best results for glacier mapping were obtained with thresholding of a TM4 by TM5 ratio image from DN, especially with respect to glacier areas in cast shadow. The accuracy is better than 3% for debris-free glacier areas. Compared to other investigated methods, this method is easy and fast to perform, needs no special image-processing software, and interactive selection of the threshold value is quite robust. The use of a median filter improves the results of the

classification by removing misclassification (small snow fields, shadow pixels) and adding pixels where needed (small debris cover, glacier parts in shadow). For glaciers smaller than 0.1 km², the glacier size is altered significantly by this noise-filter and, thus, the lower limit of total glacier area was determined to be 0.1 km² in the SGI 2000.

The new GIS-based concept of the SGI 2000 is able to compute all glacier parameters automatically. This is very useful for efficient monitoring over large areas, especially in remote regions, or to investigate small glaciers and their changes. The design of the glacier basin vector layer, which maintains the glacier identification, is not limited to the availability of a digitized glacier inventory. In remote areas without any data, creation directly from the satellite image is also possible. If a DEM is available, 3D glacier parameters (e.g. slope, aspect, hypsography) can be calculated automatically, too. For the relatively small glaciers in the Alps, a high-precision DEM with 25 m spatial resolution is necessary for obtaining glacier parameters. Useful data from other regions can also be obtained with a coarser DEM, depending on the size and characteristics of the glaciers considered.

At the moment, the main problem for the SGI 2000 is the automatic mapping of debris-covered glacier ice. It is partly included after the automatic classification (with TM4 / TM5) in two cases: the debris cover is thin or it is a medial moraine of only one pixel width (and arbitrary length). In the latter case the median filter will close the gap. Unfortunately, this automatically included part of debris-covered ice has a varying size in different years, depending on snow cover, glacier change or illumination. For this reason, only a small fraction of debris-free glaciers were chosen for comparison of glacier areas in Part II to this paper (Kääb and others, this issue). A possible solution may be the combination of advanced digital image-processing techniques (neural networks) with geomorphometric measures and object-oriented classification (Bishop and others, 2000). First promising results have been achieved by combining slope information with a map of vegetation-free areas and neighbourhood relations to glacier ice. Meanwhile, manual delineation by on-screen digitizing is applied for the SGI 2000.

ACKNOWLEDGEMENTS

The study is supported by a grant from the Swiss National Science Foundation (contract number 21-54073.98). We gratefully acknowledge the careful and constructive comments of the two anonymous referees and the editor.

REFERENCES

- Aniya, M., H. Sato, R. Naruse, P. Skvarca and G. Casassa. 1996. The use of satellite and airborne imagery to inventory outlet glaciers of the Southern Patagonian Icefield, South America. *Photogramm. Eng. Remote Sensing* **62**(12), 1361-1369.
- Bayr, K.J., D.K. Hall and W.M. Kovalick. 1994. Observations on glaciers in the eastern Austrian Alps using satellite data. *Int. J. Remote Sensing*, **15**(9), 1733-1742.
- Bishop, M.P., J.S. Kargel, H.H. Kieffer, D.J. MacKinnon, B.H. Raup and J.F. Shroder, Jr. 2000. Remote-sensing science and technology for studying glacier processes in high Asia. *Ann. Glaciol.*, **31**, 164-170.
- Environmental Systems Research Institute (ESRI). 1999. *Arc/Info 8.0.1*. Redland, CA, Environmental Systems Research Institute Inc.
- Gratton, D.J., P.J. Howarth and D.J. Marceau. 1990. Combining DEM parameters with Landsat MSS and TM imagery in a GIS for mountain glacier characterization, *IEEE Trans. Geosci. Remote Sensing*. **GE-28**(4), 766-769.
- Haeberli, W., J. Cihlar and R. Barry. 2000. Glacier monitoring within the Global Climate Observing System. *Ann. Glaciol.*, **31**, 241-246.
- Hall, D.K., A.T.C. Chang and H. Siddalingaiah. 1988. Reflectances of glaciers as calculated using Landsat 5 Thematic Mapper data. *Remote Sensing of Environment*, **25**(3), 311-321.
- Herren, E.R., M. Hoelzle and M. Maisch. 1999. *The Swiss glaciers 1995/96 and 1996/97*. Zürich, Swiss Academy of Sciences. Glaciological Commission; Federal Institute of Technology. Laboratory of Hydraulics, Hydrology and Glaciology. (Glaciological Report No. 117/118).
- Jacobs, J.D., E.L. Simms and A. Simms. 1997. Recession of the southern part of Barnes Ice Cap, Baffin Island, Canada, between 1961 and 1993, determined from digital mapping of Landsat TM. *J. Glaciol.*, **43**(143), 98-102.
- Kääb, A. 2001. Photogrammetric reconstruction of glacier mass balance using a kinematic ice-flow model: a 20 year time series on Grubengletscher, Swiss Alps. *Ann. Glaciol.*, **31**, 45-52.
- Kääb, A., F. Paul, M. Maisch and M. Hoelzle. (in press). The new remote sensing derived Swiss glacier inventory: II. Results. *Ann. Glaciol.*, **34**.
- Kargel, J. S. 2000. New Eyes in the Sky Measure Glaciers and Ice Sheets. *EOS, Transactions of the American Geophysical Union*. **81**(24), 265, 270, 271.
- Maisch, M., A. Wipf, A., B. Denzler, J. Battaglia and C. Benz. 1999. *Die Gletscher der Schweizer Alpen. Gletscherhochstand 1850, Aktuelle Vergletscherung, Gletscherschwund-Szenarien*, vdf Hochschulverlag, ETH Zürich, Schlussbericht NFP31, 373 S.
- Müller, F., T. Cafilisch and G. Müller. 1976. *Firn und Eis der Schweizer Alpen: Gletscherinventar*, Zürich, Eidgenössische Technische Hochschule. (Geografisches Institut Publ 57.)
- Paul, F. In press a. Evaluation of different methods for glacier mapping using Landsat TM. *20th EARSeL Symposium, 16-17 June 2000, Dresden. Proceedings*.
- Paul, F. In press b. Changes in glacier area in Tyrol, Austria, between 1969 and 1992 derived from Landsat 5 TM and Austrian Glacier Inventory data. *Int. J. Remote Sensing*.
- Rott, H. 1994. Thematic studies in alpine areas by means of polarimetric SAR and optical imagery, *Adv. Space Res.*, **14**(3), 217-226.
- Serandrei-Barbero, R., R. Rabagliati, E. Binaghi and A. Rampini. 1999. Glacial retreat in the 1980s in the Breonie, Aurine and Pusteresi groups (eastern Alps, Italy) in Landsat TM images. *Hydrol. Sci. J.*, **44**(2), 279-296.
- Sidjak, R.W. and R.D. Wheate. 1999. Glacier mapping of the Illecillewaet icefield, British Columbia, Canada, using Landsat TM and digital elevation data. *Int. J. Remote Sensing*, **20**(2), 273-284.

FIGURES

Fig. 1. Location of the test area, the 'Weissmies' group of mountains in Switzerland (see inset), and as seen with Landsat TM (band 3) on 12. September 1985 (contrast enhanced). Black lines indicate the glacier outlines from the digitized glacier inventory of 1973. Size of imagery is about 15 km by 15 km. Landsat TM data: © Eurimage.

Fig. 2. Glacier masks comparing two methods at a time. Areas in light grey were identified by both methods as being a glacier, dark grey areas only by the first method, and black areas only by the second method. The compared methods are: a) TM 3 / TM 5 and TM 4 / TM 5 from DN, b) as a) but all TM bands from at satellite planetary reflectance, c) with an unsupervised ISO-DATA clustering (20 clusters) algorithm and TM 4 / TM 5 from DN d) with a supervised Maximum-Likelihood classification of training areas with 8 classes and TM 4 / TM 5 from DN.

Fig. 3. Cavagnoli (C) and Basodino Glacier (B) with outline from TM (black) from 15. September 1992 and the Swiss glacier inventory from 1973 (white) on a SPOT Pan scene from 17. September 1992. This area (size about 5 by 7 km) is located 45 km NE of the test area 'Weissmies'. SPOT data: © SPOT Image.

Fig. 4a. Illuminated version of the DEM used for the SGI 2000 in a sub-section of the test area 'Weissmies' with outlines of 7 glaciers (numbered) from the digitized inventory of 1973. DEM artefacts are clearly visible. Fig. 4b. Differences in slope between the DEM in Fig. 4a and a reference DEM ranging from -53° (black) to $+65^{\circ}$ (white). Most of the artefacts are located outside of glacier areas. Elevation data: DEM 25 © Swiss Office of Topography (BA013305).

Fig. 5. Glacier basins (bold black lines) and the digitized Swiss glacier inventory of 1973 (grey areas). Contiguous ice masses were separated into individual glaciers according to the 1973 inventory, and roughly surrounded to obtain closed polygons. These polygonal glacier basins can also be used for elimination of gross classification errors (e.g. pro-glacial lakes) and for glacier identification, especially to assign a unique ID to glaciers.

Fig. 6. Work flow between sequential modules and principal data flow within each module. In each module different programs are available for calculation of glacier parameters and their changes. Most of them can be combined to a complete digital processing chain.

Fig. 7. The principal data flow within the GIS-module using Arc/Info and including a DEM product for 3D glacier parameters. Areas of individual glaciers are available after step 2.

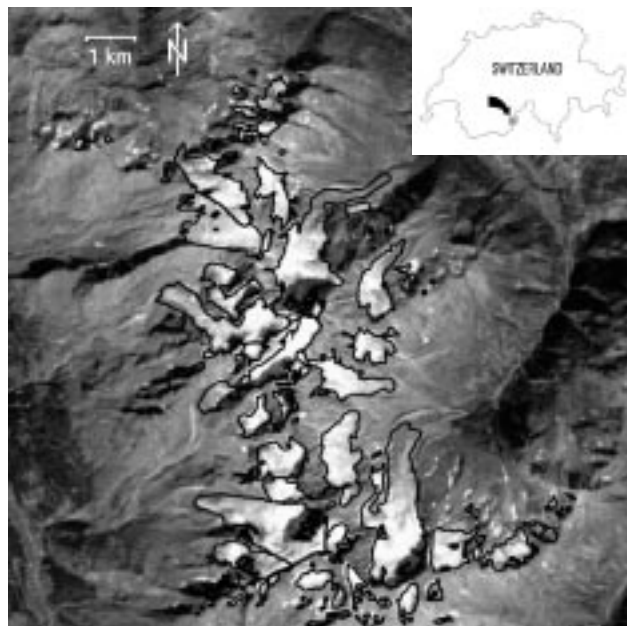


Figure 1

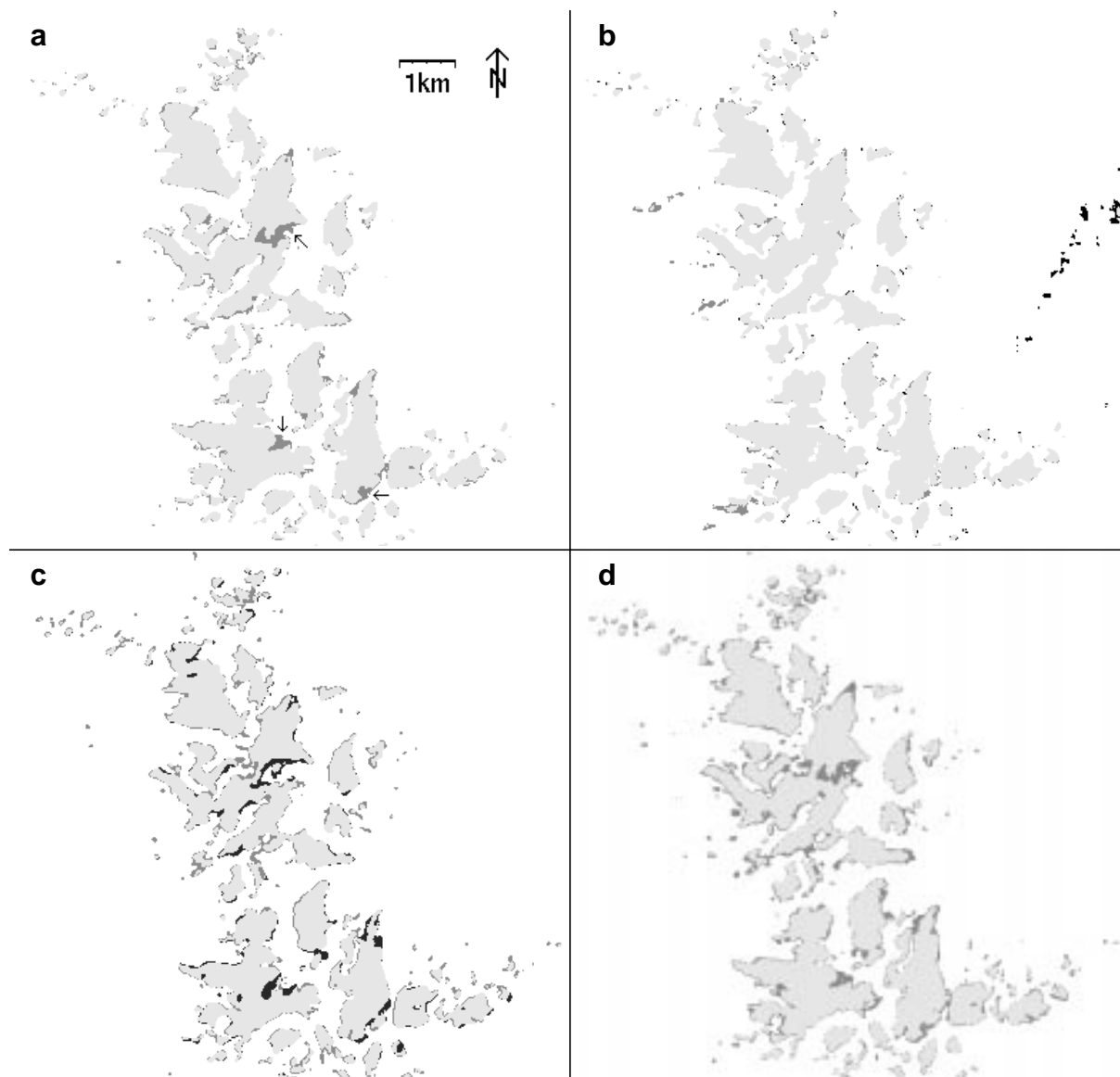


Figure 2

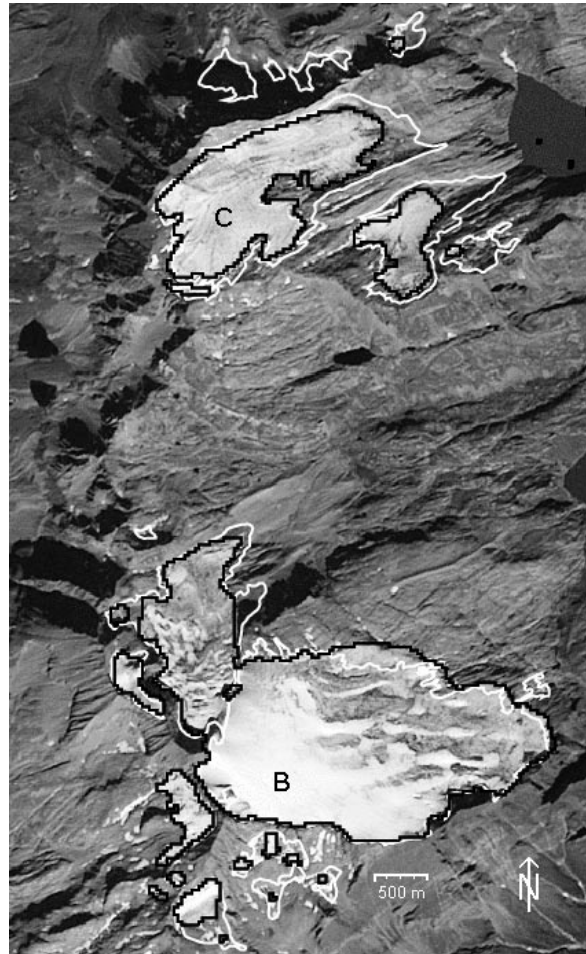


Figure 3

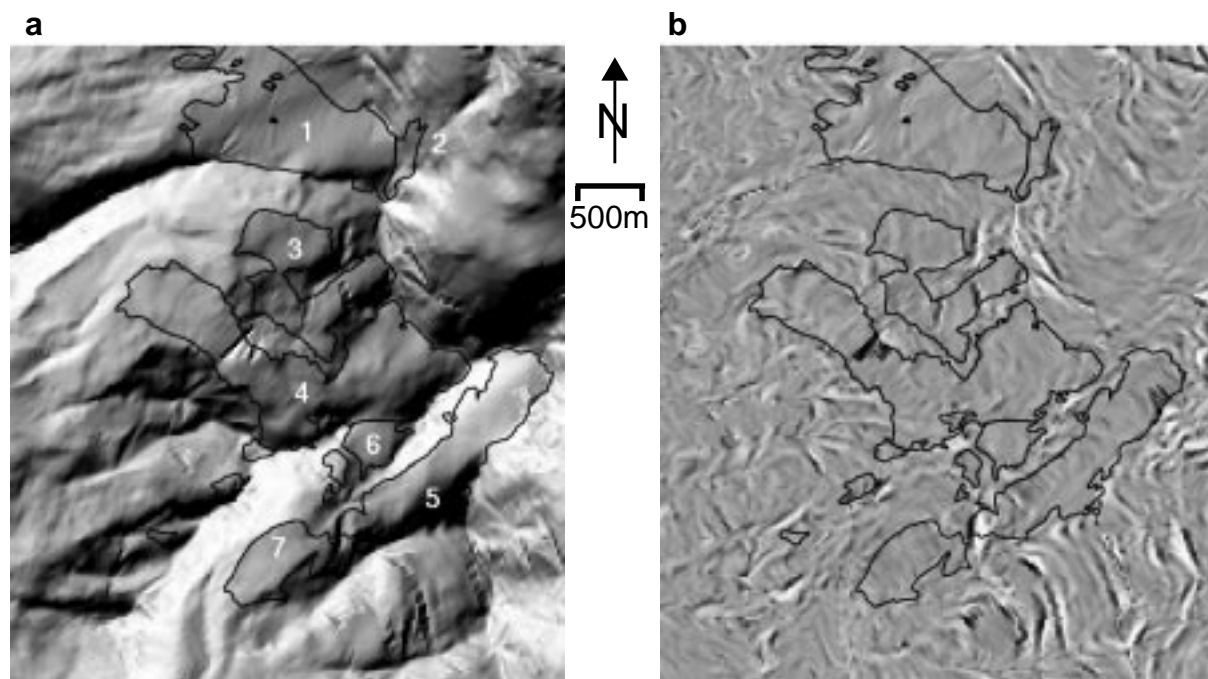


Figure 4a and 4b



Figure 5

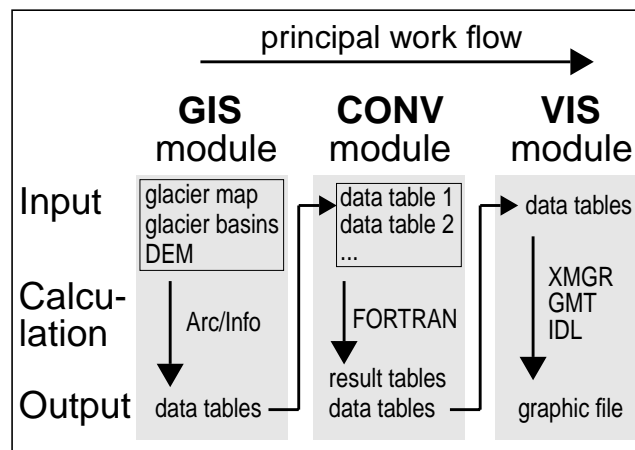


Figure 6

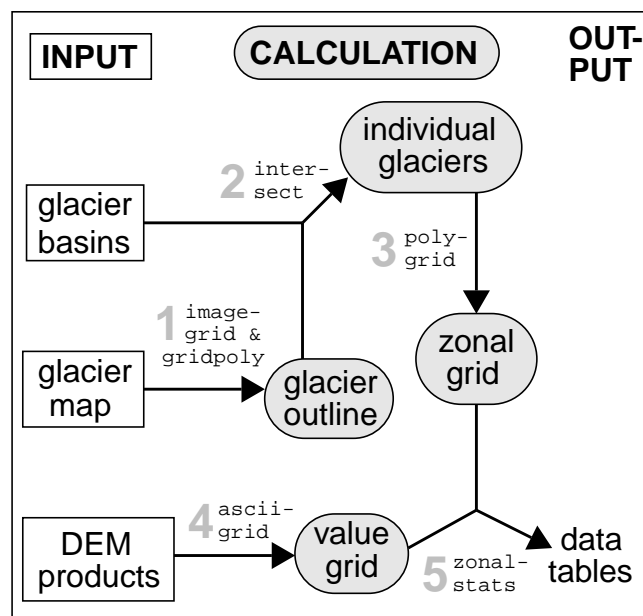


Figure 7